

Supplementary information

Renewable Hydrogen Generation from a Dual-Circuit Redox Flow Battery

Véronique Amstutz^a, Kathryn E. Toghil^a, Francis Powlesland^a, Heron Vrubel^b, Christos Comninellis^a, Xile Hu^b, and Hubert H. Girault^{a,*}

Ecole Polytechnique Fédérale de Lausanne, EPFL-SB-ISIC-LEPA, Station 6, 1007 Lausanne, Switzerland.

Hubert.Girault@epfl.ch

Fax: +41 21 693 36 67, Tel: +41 21 693 31 51

^bEcole Polytechnique Fédérale de Lausanne, EPFL-SB-ISIC-LSCI, BCH 3305, Lausanne, Switzerland.

1. Cyclic voltammetry for V(III)/V(II) and Ce(IV)/Ce(III)

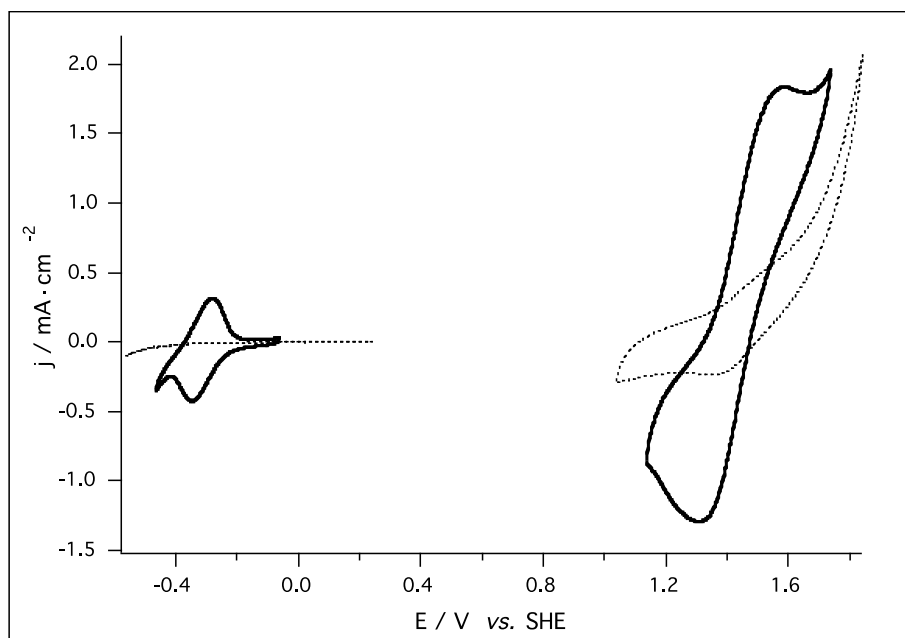


Figure S1: Cyclic voltammograms of 50 mM vanadium(IV) sulfate and 50 mM cerium(III) sulfate in 1 M H₂SO₄ (-) and 1 M H₂SO₄ (--) background signal on a graphite polymer rod electrode.

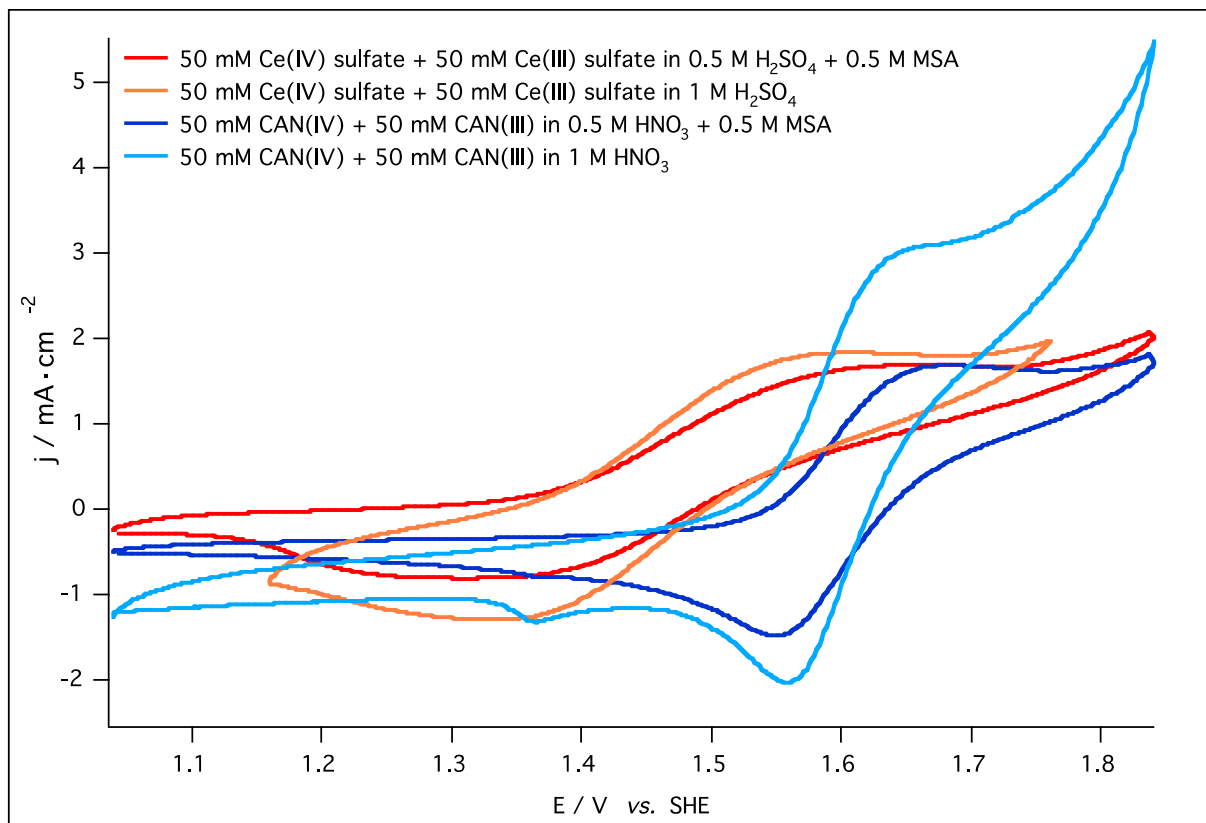


Figure S2: Comparison of the Ce(IV)/Ce(III) redox couple electrochemical behaviour in nitric acid, nitric acid/MSA, sulfuric acid and sulfuric acid/MSA media at 20 mV/s on a graphite rod electrode.

2. Charging and discharging curves for the Ce-V RFB

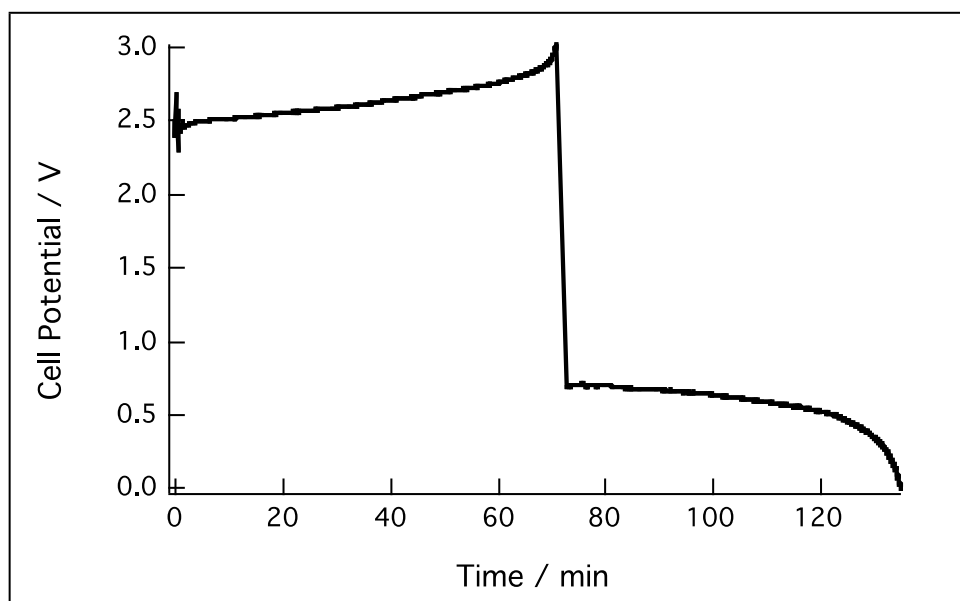


Figure S3: Galvanostatic charging and discharging curves for 100 mM Ce(IV) sulfate (anolyte) and 100 mM VCl_3 (catholyte) solutions. Conditions: 1 M H_2SO_4 , 60 mA/cm^2 , 2 cm^2 graphite felt electrodes.

3. UV-vis spectra of V(II) and V(III)

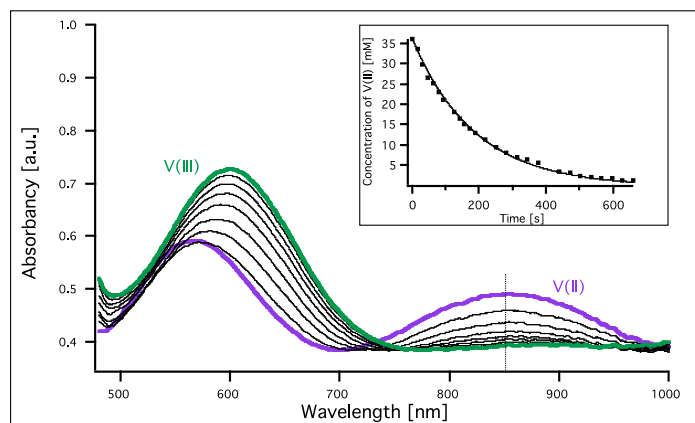


Figure S4: UV-vis spectra of a solution of 40 mM V(II) as a function of time in presence of 1 mg Mo₂C. After 660s, it has been totally converted to V(III) (green curve). The inset represents the concentration of V(II) as a function of time (dots), and the recalculated concentration of V(II) from the obtained rate law (line).

4. Details on the kinetic calculations

4.1. Kinetic calculations for the reaction of hydrogen generation

The considered reaction is reaction (3) of the main text. In order to determine the kinetic parameters, the V(II) consumption was followed as a function of time by measuring the UV-vis V(II) peak change at 850.45 nm. The baseline was subtracted to this value, as it was fluctuating during the reaction, due to bubble formation and the presence of the catalytic powder. The solution was strongly mixed during the whole experiment. The V(II) peak value was compared to a calibration curve to obtain the concentration of V(II) in the sample as a function of time.

To determine the reaction order, this plot was fitted with an exponential fit for the first 3 minutes of the experiment using Mathematica. The natural logarithm of the derivative of this fitting expression was then plotted against the natural logarithm of the concentration according to the following relation:

$$\ln v = a \ln C_{V^{2+}} + b$$

Slope a on this plot represents the order of the reaction for V(II). It was determined for multiple experiments and was close to 1.

In order to determine the apparent rate constant k_{app} for the considered reaction, knowing that the reaction is first order regarding V(II), the following integrated rate law

was used with the experimental V(II) concentrations at time t $C_{V^{2+}}^t$ and the initial concentration of V(II) $C_{V^{2+}}^{\text{initial}}$:

$$-k_{\text{app}} t = \ln \left(\frac{C_{V^{2+}}^t}{C_{V^{2+}}^{\text{initial}}} \right)$$

The acid concentration and the amount of catalyst also affected the rate of reaction evidenced by multiple experiments where both were varied. This implies that both species are also involved in the rate-determining step of the reaction. Further research will be conducted to further understand the mechanism.

4.2. Kinetic calculations for the reaction of water oxidation

The water oxidation reaction is described in equation (4) of the main text. Only the effect of Ce(IV) concentration has been evaluated here. This reaction has previously been evaluated in other work on RuO₂ catalysts or IrO₂ catalysts^{1,2}.

The kinetics were determined by following the amount of oxygen produced in the headspace (the amount of oxygen dissolved was calculated but appears to be negligible compared to the amount of oxygen in the headspace), which was measured by a fluorescent probe. The signal of the probe depends both on the percentage of oxygen in the atmosphere, and on the pressure build-up inside the vessel, as it was calibrated at ambient pressure.

To calculate the partial pressure of oxygen in the headspace pO_2 , it was assume that initially, only nitrogen gas, at a pressure of 1 atm ($pN_2^{\text{initial}} = 1 \text{ atm}$) was present in the headspace and that the amount of vapour is negligible ($pH_2O = pH_2O^{\text{initial}} = 0 \text{ atm}$). The vapour pressure of water at 25°C is 3.16 kPa³, which is low compared to the partial pressures of nitrogen and hydrogen in the headspace. This led to the following third degree polynomial that has to be solved in order to obtain the number of moles of oxygen produced from the oxygen percentage:

$$0 = (2 - S) \cdot pO_2^3 + ((3 - 3 \cdot S) \cdot pN_2^{\text{initial}}) \cdot pO_2^2 + ((1 - 3 \cdot S) \cdot (pN_2^{\text{initial}})^2) \cdot pO_2 - S \cdot (pN_2^{\text{initial}})^3$$

Where S is the signal (percentage of oxygen) given by the probe/100. The polynomial was solved for each value of the signal measured with Mathematica, leading to a partial pressure for oxygen for each second, at least.

In order to calculate the corresponding number of moles of oxygen n_{O_2} , the ideal gas law was assumed and the following formula was therefore used:

$$n_{O_2} = \frac{p_{O_2} \cdot V_{\text{headspace}}}{0.082 \cdot T}$$

Where $V_{\text{headspace}}$ is the volume of the headspace [L], 0.082 is the gas constant [L·atm·mol⁻¹·K⁻¹] and T is the ambient temperature [K].

In order to calculate the number of moles of cerium that was consumed at each time, we used the amount of oxygen produced and the conversion efficiency presented in the main text, that is about 78 %, knowing that the stoichiometry of the reaction dictates that 4 moles of Ce(IV) are required to produce 1 mole of oxygen.

The kinetics was then determined exactly the same way as for the reaction of hydrogen evolution, described above. This is because we also obtained a unit order of reaction towards Ce(IV), and thus the same integrated rate law can be used.

5. Detailed calculation of the overall efficiency of the system

The calculation of the efficiency for the conversion of electricity to hydrogen is based on the comparison between the energy input (*i.e.* the total energy required for fully charging the V–Ce RFB) and the energy output (*i.e.* the energy contained in the produced hydrogen gas based on its combustion). The following data were used:

- Charging current density: $j = 60 \text{ mA}\cdot\text{cm}^{-2}$
- Electrode area: $A = 2 \text{ cm}^2$
- Full charge time: $t_{\text{ch}} = 70 \text{ min}$
- Volume of the solutions: $V = 50 \text{ mL}$
- Concentration of the electroactive species (Ce(III) and V(III)): $C = 0.1 \text{ mol}\cdot\text{L}^{-1}$
- Mean charging voltage: $E_{\text{ch}} = 2.5 \text{ V}$
- Lower heating value for hydrogen: $LHV = 241 \text{ kJ}\cdot\text{mol}^{-1}$
- Yield of the catalytic reaction for hydrogen generation: $Y = 100 \%$

The energy required to fully charge the battery is calculated as follows:

$$E_{\text{in}} = E_{\text{ch}} \cdot j \cdot A \cdot t = 1260 \text{ J}$$

The energy contained in the hydrogen produced is:

$$E_{\text{H}_2} = LHV \cdot C \cdot V = 603 \text{ J}$$

The overall efficiency is therefore:

$$\eta_{\text{overall}} = \frac{E_{\text{H}_2}}{E_{\text{in}}} \cdot 100 = 48\%$$

It is worth noting that the energy of the pumping system was not including in the calculation and it would significantly decrease the efficiency for such a small system. However, for larger installations, the pumping energy cost would become less significant. Additionally, the compression of the produced hydrogen gas would also require some energy.

6. Study of IrO₂ as catalyst for the reaction of water oxidation

6.1. Synthesis of IrO₂ and deposition on silica microparticles

The IrO₂ catalyst was prepared as follows. 50 mL of IrO₂ nanoparticles were synthesised from K₂IrCl₆ (99% metal basis, Sigma-Aldrich) according to the procedure outlined by Hara *et al.*⁴. IrO₂ nanoparticles were characterised by UV-vis measurement (peak at 590 nm). They were then electrostatically deposited on silica particles, by first coating the silica with poly(diallyldimethylammonium chloride) (PDDA) giving a positively charged surface. 0.8 g of SiO₂ (SilicaFlash P60, SilicaCycle), 0.8 g of NaCl (Fluka), and 400 µL of PDDA (20% in water, average MW: 100 000-200 000 Da, Aldrich) were added to 20 mL of deionised water. The solution was stirred at room temperature for 1h then centrifuged (15 minutes, 8000 tours/minute, Biofuge Stratos, Heraeus). The supernatant was then removed, the solid washed with deionised water and centrifuged again. This process was repeated twice more. The coated silica was then dried at 80°C for 10 minutes on a filter paper. 0.4 g of the coated silica was added to 50 mL of the solution containing the suspended IrO₂ nanoparticles, and the solution was mixed for 2h. The suspension then also underwent centrifugation and washing as before, 3 times. The now purple powder was then filtrated and dried on a filter paper for 10 min at 80°C. It was used as a catalyst in further experiments in the powder form.

6.2. Study of the activity of $\text{IrO}_2/\text{SiO}_2$ in various acidic media

As mentioned in the main text, the standard reduction potential of Ce(IV) depends on its coordinated ligands, and thus on the initial salts and the acidic media. Moreover, Pletcher *et al.*⁵ have suggested that the sulfate ions are more strongly coordinated to the cerium ions than the nitrate ions. These authors also showed that the redox potential was lower for the cerium sulfate than for the cerium nitrate. Here we also study the methanesulfonic acid media. For the three acids, the Ce(IV) ions is thermodynamically capable of oxidizing water to oxygen, but it not observed in absence of catalyst.

When $\text{IrO}_2/\text{SiO}_2$ was added, the conversion of Ce(IV) to Ce(III) and the generation of oxygen was clearly visible in nitrate and methanesulfonic acid media, but did not occur in the sulfate medium. However, when the sulfate media was mixed with methanesulfonic or nitric acid, the reaction may occur, but only when the concentration of sulfate was much lower than the one of nitric acid or methanesulfonic acid (*e.g.* 1 : 4 H_2SO_4 : HNO_3). It may indicate that the number of sulfate ligands on the cerium ion affects its reduction potential and/or its ability to be an electron acceptor in the oxidation of water.

6.3. Study of the effect of the amount of catalyst on the rate of generation of oxygen

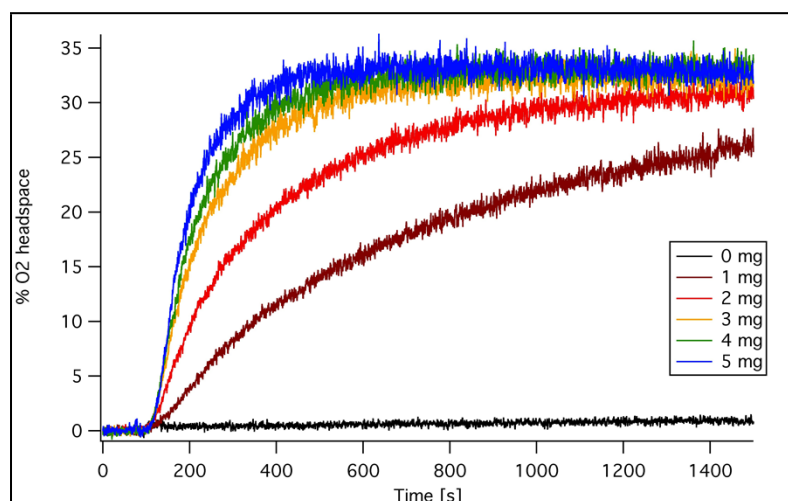


Figure S5: Effect of the catalyst mass on the amount of oxygen produced in stirred shake-flask. Conditions: 2 mL of 100 mM CAN(IV) in 0.5 M HNO_3 + 0.5 M MSA, at 25°C. The mass of $\text{IrO}_2/\text{SiO}_2$ varied between 0 and 5 mg. The experiment was done under nitrogen atmosphere and the amount of oxygen was detected by a fluorometric probe.

7. RuO₂ kinetics

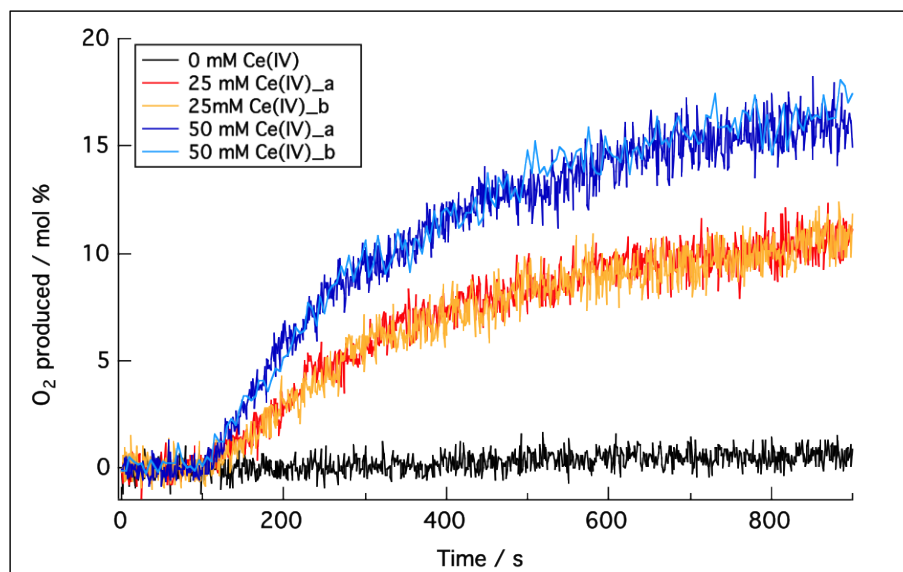


Figure S6: Kinetic determination of the reaction of water oxidation. 2mL of 0, 25 mM, and 50 mM of Ce(IV) sulfate solutions were mixed under a nitrogen atmosphere during 900 s, in presence of 0.5 mg of heat pre-treated RuO₂. The build-up of oxygen gas in the headspace of the 4.8 mL flask is measured using a fluorescent probe.

8. Picture of the electrochemical cell of the cerium-vanadium redox flow battery (V-Ce RFB)/ Design of the V-Ce RFB electrochemical cell

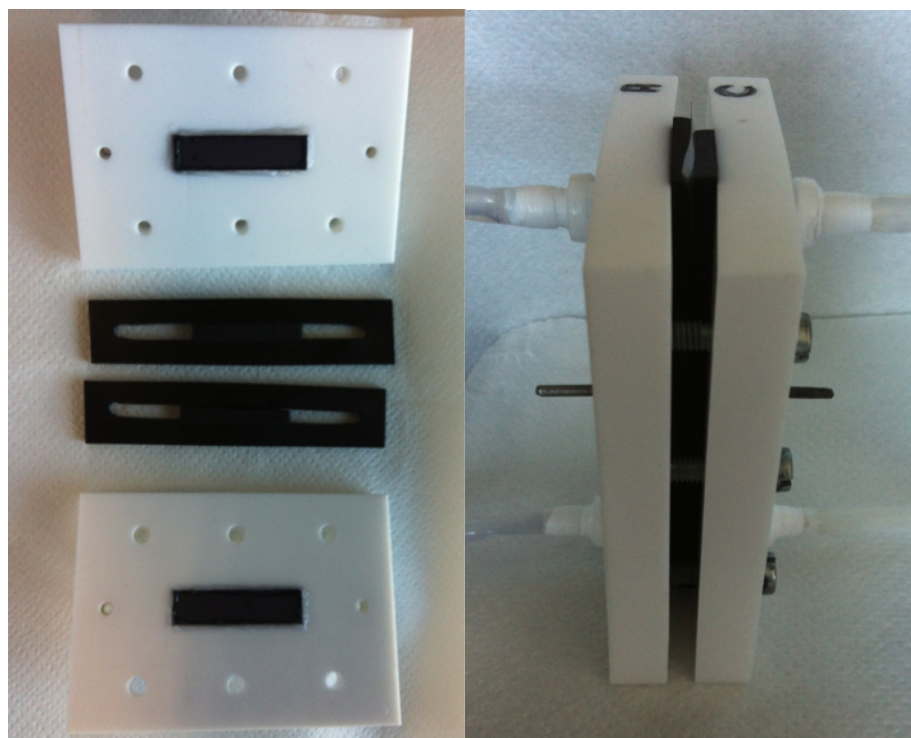


Figure S7: Picture of the laboratory scale electrochemical cell used in the present system.

9. References SI

- 1 N. C. King, C. Dickinson, W. Zhou and D. W. Bruce, *Dalton Transactions*, 2005, 1027-1032.
- 2 D.B. Grotjahn, D.B. Brown, J.K. Martin, D.C. Marelius, M.-C. Abadjian, H.N. Tran, G. Kalyuzhny, K.S. Vecchio, Z.G. Specht, S.A. Cortes-Llamas, V. Miranda-Soto, C. van Niekerk, C.E. Moore and A.L. Rheingold, *The Journal of the American Society*, 2011, 133(47), 19024-19027.
- 3 E. W. Lemmon, Vapor pressure and other saturation properties of water in *CRC Handbook of Chemistry and Physics*, 94th Edition, W. M. Haynes, 2013, <http://www.hbcpnetbase.com/>.
- 4 M. Hara, C. C. Waraksa, J. T. Lean, B. A. Lewis and T.E. Mallouk, *The Journal of Physical Chemistry A*, 2000, 104, 5275-5280.
- 5 D. Pletcher and E. Valdes, *Electrochimica Acta*, 1988, 33, 499-507.